Detection of osteoarthritis in knee and hip joints by FFC NMR

Lionel M. Broche[1*], George P. Ashcroft[2], David J. Lurie[1]

[1] Aberdeen Biomedical Imaging Centre, School of Medical Sciences, University of Aberdeen, UK; [2] School of Medicine & Dentistry, University of Aberdeen, UK
Corresponding author: l.broche@abdn.ac.uk

Abstract

It is known that in the early stages of osteoarthritis (OA) the concentration of glycan proteins decreases in articular cartilage. This phenomenon is under active research to develop a means to characterise OA accurately in the early stages of the disease, when still reversible. However, no method of quantification has yet shown clear success in this area. In this paper we propose a novel approach to detect glycan depletion using Fast Field-Cycling NMR (FFC NMR). This technique was previously reported to allow non-invasive measurement of protein concentration via the ^{14}N quadrupolar relaxation in certain amide groups. We have demonstrated that articular cartilage exhibits clear quadrupolar peaks that can be measured by a benchtop FFC NMR device and which changes significantly between normal and diseased tissues ($p < 0.01$). This signal is probably glycan-specific. The method may have potential for early evaluation of OA in patients on FFC-MRI scanners currently under evaluation in the authors' laboratory.

Keywords

Fast field-cycling NMR, early detection of osteoarthritis, pilot study, ^{14}N quadrupolar cross-relaxation.

Word count: 3736

Introduction

Articular cartilage provides the low-friction, gliding surface of human synovial joints (e.g. knee and hip) and is relatively wear-resistant under normal circumstances (1). It is a layer 2 - 4 mm thick that covers the contact surfaces between bones and comprises 70 - 80% water and 20 - 30% protein, mainly collagen and glycan, the exact composition varying within the different layers of the cartilage and between joints and sites on an articular surface (2).

Osteoarthritis (OA) is a disease that affects cartilage. It is the most common cause of disability in the United Kingdom (UK): and in 2003, OA was estimated to affect 9.6% of men and 18% of women over 60 years old worldwide (3). Interest in developing potential therapeutic agents has highlighted the need for new biomarkers of disease progression, with imaging biomarkers currently appearing to offer the best prospect.

Traditional radiographs, using joint space narrowing on weight-bearing x-rays have been used as a surrogate marker for structural change for many years by regulatory agencies such as the FDA (4). However, the poor sensitivity of the technique means that recently research has concentrated on other imaging modalities with the main one being MRI assessment of cartilage (5, 6). Three forms of assessment are in current use, as follows:

Morphological change: where specific features such as focal cartilage loss, bone lesions and other damages can be identified.

Quantitative MR imaging of cartilage: both semi-automated and fully-automated methods have been used to measure changes in articular cartilage volume over time with good repeatability and precision.

Surrogate markers of cartilage composition: Diseased cartilage is depleted of certain glycosaminoglycans (GAG) and collagen at an early stage of development of OA (7). Several MRI techniques have been used to detect these variations, mainly sodium imaging (8), delayed gadolinium-enhanced MRI of cartilage (dGEMRIC), $T_{1\rho}$ imaging, T_2 imaging (9) and magnetisation transfer (10), each having its advantages and drawbacks.

Recent works (11, 12) have demonstrated the superiority of T_1 over other MR parameters to characterize cartilage matrix. Here we propose a novel approach for the measurement of glycan depletion in OA from T_1 measurement using Fast Field-Cycling NMR (FFC NMR). This technique is similar to conventional NMR but allows measurement of relaxation times at a wide range of Larmor frequencies by changing the main magnetic field. The principles of FFC-NMR were first described in 1951 (13), applied to various materials (14), first translated to imaging for the study of free radicals (15) and have been followed by a number of imaging applications (16, 17). Our research unit has developed four FFC MRI scanners using permanent and/or resistive magnets, with various applications in unconventional imaging techniques such as free radical imaging, magnetisation transfer (18) or ^{14}N quadrupolar cross-relaxation imaging (16).

Theory

Field-cycling techniques allow the measurement of T_1 at a range of magnetic fields, using a single instrument. Variations in the T_1 dispersion curve can be linked quite directly to physical properties such as diffusion, porosity or others (14, 19). Our work focuses on a particular feature of the T_1 dispersion curve, the ^{14}N quadrupolar peaks, which originate from cross-relaxation when the Zeeman energy of ^{1}H matches one of the nuclear quadrupolar transitions of ^{14}N nuclei (20). [14]N nuclei relax quickly via their quadrupolar moment and provide an additional relaxation pathway to bulk water protons. In an FFC experiment, this transfer of magnetisation can be controlled by adjusting the evolution field and results in three 'peaks' in the R_1 dispersion curve at positions given by:

$$\omega_1 = \omega_Q \left(3 - \eta\sqrt{1+a^2}\right)/4$$

$$\omega_2 = \omega_Q \left(3 + \eta\sqrt{1+a^2}\right)/4 \qquad [1]$$

$$\omega_3 = \omega_Q\, \eta\, \sqrt{1+a^2}\, /2$$

With:

$$a = \frac{4\,\omega_N \cos\theta}{\omega_Q\, \eta} \qquad [2]$$

where ω_Q is the quadrupole coupling constant, η is the asymmetry parameter, ω_N is the Zeeman coupling constant of ^{14}N and θ is the angle between the magnetic field and the main axis of the molecular frame, taken along the direction of the largest eigenvector of the quadrupolar tensor (21). Biological samples are not crystalline so θ is averaged over all directions of space. This gives quadrupolar peaks wider than in crystals (typically 0.4 MHz ^{1}H width) and centred around 0.7, 2.1 and 2.8 MHz ^{1}H frequency (or 16, 49 and 65 mT), which correspond to a quadrupolar coupling constant of 3.3 MHz from Eq. 1. That is much larger than the [14]N Larmor frequency at the same fields (50 - 200 kHz) and allows use of the low-field approximation so that $a \approx 0$ from Eq. 2.

While the exact origin of the quadrupolar peaks is not certain, physical considerations suggest that it originates from amide groups (22). Even though most proteins contain amide groups, not all of them show quadrupolar peaks. Several conditions are necessary for the transfer of magnetisation from a dipole to a quadrupole: the protein motion must be restricted (gel or solid phase) and the amide group should attract water molecules with a residence time long enough to allow magnetisation transfer but also short enough to relax a large number of water protons (typically about 1 μs) (22). Some proteins, such as *in vitro* collagen, do not show quadrupolar peaks whereas others do, such as bovine serum albumin. These factors contribute to make quadrupolar cross-relaxation quite specific.

Another important characteristic of quadrupolar cross-relaxation is that each ^{14}N site contributes independently to the cross-relaxation so that the overall amplitude taken from the R_1 dispersion curve is proportional to the concentration of contributing sites (19). We can therefore exploit this linearity, together with the specificity of the quadrupolar cross-relaxation mentioned above, to measure the concentration of GAG in cartilage tissues and check if this method is sensitive enough to detect OA. In practice the relaxation rate is the sum of the quadrupolar cross-relaxation rate and the spin-lattice relaxation rate so we can obtain an estimate of the pure quadrupolar peaks by subtracting the background relaxation curve and then integrating the residuals.

Methods

Samples of cartilage were obtained during hip or knee surgery and patients were evaluated from clinical history and an X-ray diagnosis made using the grading proposed by Kellgren and Lawrence (23). Samples were considered healthy at grade 0 and diseased at grade 3. Grade 4 was not considered because of the small amount of material available. Table 1 shows a summary of the patients included. Ethical approval for the study was granted by the North of Scotland Research Ethics Committee.

Osteoarthritis samples: patients undergoing hip or knee replacement for primary osteoarthritis were identified prior to surgery, recruited to this pilot study and informed consent was obtained. 23 samples were derived from 5 patients at the time of surgery following removal of the femoral head (in hip replacement) or the femoral and tibial articular surfaces (in knee replacement). The samples were taken from the visible remaining articular cartilage.

Normal samples: Informed consent was obtained from patients undergoing hip replacement for osteoporotic fractured neck of femur with no preceding osteoarthritis of the hip observed from clinical history or radiographs. 26 samples were derived from 7 patients at the time of surgery following removal of the femoral head. The samples were taken over the whole articular surface.

Between four and eight samples were taken from each patient with total volumes of 0.2 to 1 cm^2 each. Samples were usually transported for analysis on the day of surgery. When necessary, some samples were kept at 4°C before they could be analysed. The samples were placed in NMR tubes and analysed by FFC NMR using a SMARTracer relaxometer (Stelar s.r.l., Italy). The R_1 dispersion curve was measured by inversion recovery at fields between 0.05 and 7 MHz proton Larmor frequency, with a finer sampling in the regions 0.4-0.9 MHz and 1.5 - 3.5 MHz where the quadrupolar peaks were expected. R_1 values at each evolution field were measured using 6 repeats of 12 measurements taken linearly in time. The polarisation time, polarisation field and acquisition field were set to 0.5 s, 8 MHz and 7.4 MHz respectively. The samples were kept at 37°C during acquisition.

The data processing was performed with Matlab r2009a with the curve fitting toolbox (Mathworks Inc.), and Octave 3.2.4 (www.gnu.org/software/octave) for the Pearson's

product moment correlation test. The curve fitting algorithm estimated R_1 values from the absolute magnitude data using an absolute-valued monoexponential decay model. This prevented problems with phase detection for points that were close to zero magnitude, which was a common problem for this pulse sequence with the relaxometer used. The R_1 dispersion curve was divided into background and quadrupolar peaks by curve fitting: the background was fitted using a bi-Lorentzian model, which was found empirically to fit closely to the background data over 4 decades in frequency with 5 parameters, and the quadrupolar peaks were fitted using a recent model of quadrupolar relaxation in proteins (22). The quadrupolar relaxation model requires a relatively large number of parameters so we estimated the amplitude of the peaks separately by numerical integration of the pure quadrupolar peaks, found by subtraction of the background, between 0.4 and 3.5 MHz.

The scripts of the fitting routine were kindly provided by Professor Bertil Halle (Department of Biophysical Chemistry, Lund University, Sweden) with minor alterations for convenience. This algorithm models quadrupolar peaks by processing the convolution of the quadrupolar cross-relaxation peaks with the orientation function that models the different orientations of the NH bonds relative to the main magnetic field (22).

Results

Figure 1 shows two typical inversion recovery curves from healthy and diseased samples, taken randomly in the data set. The R^2 values from the absolute-valued monoexponential model were typically above 0.998 so that model was considered appropriate. The order of magnitude of R_1 for the samples analysed was 0.1 s^{-1}. Figure 2 shows the evolution of R_1 between 0.4 and 3.5 MHz proton Larmor frequency for typical samples of healthy and OA cartilage: the quadrupolar peaks are easily visible around 0.7, 2.1 and 2.8 MHz for both samples. The fit of the overall signal (background and peaks) is also satisfactory with R^2 values typically above 0.98.

The pure quadrupolar peaks, denoted ΔR_1, (Figure 3) were obtained by subtracting the fitted background from the R_1 dispersion curve and presented a clear difference in between the two groups. Normal probability plots suggested that the data obeyed a normal distribution (data not shown). The data regrouped by patient, on Figure 4,

shows a distinct difference between the two populations even though patient OA6 showed results significantly higher than its group, probably because two of its four samples gave integrated amplitudes above 4 MHz s^{-1}. This may be due to the inhomogeneous distribution of OA cartilage so that relatively healthy regions may have been probed.

The average cumulated amplitude of the quadrupolar peaks obtained from OA samples was lower than that from normal samples by 65% with values of 4.5 ± 1.0 and 2.8 ± 0.5 MHz s^{-1} for normal and diseased patients respectively. A t-test gave a *p*-value < 0.01, and a threshold at 3.35 MHz s^{-1} could separate the two populations with only one outlier.

The dispersion curves shown in Figure 2 also exhibit an offset between healthy and diseased cartilage that was observed consistently through all the samples. This effect was measured by averaging the raw R_1 data between 0.4 and 3.5 MHz. The average relaxation rate values measured for normal and OA samples were 13.0 ± 1.2 and 9.2 ± 0.7 s^{-1} respectively, giving a *p*-value < 0.01. The results are presented in Figure 5: a threshold of 10.7 s^{-1} gave complete separation. The Pearson's product moment correlation test also showed that the changes observed were significantly correlated to the K-L test values (*p*-values <0.01 in both cases) as seen on Figure 6.

The model used to fit the quadrupolar peaks also showed less significant changes, particularly for the quadrupolar parameters η and ω_Q from Eq.1 and for α, the angle between the NH bond and the secondary axis of the quadrupolar moment. The results obtained from the fit for these values are shown in Table 2 for normal and OA cartilage with the corresponding *p*-values.

Discussion

The quadrupolar peaks appeared clearly in all the samples analysed so at least one of the main constituents of cartilage provides quadrupolar relaxation. The most common constituents of cartilage are collagen, chondroitin sulphate, dermatan sulphate, keratin sulphate and hyaluronic acid (2, 24), but collagen does not show quadrupolar peaks *in vitro*. Also, the characteristics of the quadrupolar moment obtained on Table 2 correspond with the amide groups found in proteins, as expected (22).

We could detect two significant changes in the dispersion curve, namely a shift of the average R_1 together with variations of amplitude of the pure quadrupolar peaks. Even though the average R_1 seems to provide more robust results, it is linked to spin-lattice relaxation mechanisms that are hard to characterise in biological samples and it is not known if this variation is specific, nor if it occurs at early stages of OA. On the other hand, variations in the quadrupolar peaks appeared less robust but are closely linked to the biochemistry of the sample, are quantitative and are likely to change at early stages of OA. It can also be noted that the outlier points in the OA data set degrades the quality of the data and that if that point is ignored a complete separation of the populations is possible. Therefore both parameters should be investigated in future experiments.

We suspect that outliers appeared for the following reasons: natural spatial variations in protein depletion in diseased cartilage; undersampling of the dispersion curve; samples drying during the experimentation. These problems can be addressed by several means: higher sampling in the quadrupolar region, protection from drying (using Fluorinert to cover samples for instance), or using a healthy zone in the cartilage as a reference (especially in imaging techniques). Sample drying would not be an issue with whole body scans of patients so fewer variations are expected from FFC-MRI patient scans.

The changes observed in the amplitude of the quadrupolar peaks between healthy and OA samples are known to be proportional to the protein content (19), hence the results obtained here suggest a decrease in protein content of 35% in OA cartilage compared to healthy tissues. It was not possible to quantify protein content during this preliminary study, but our results correspond to data published previously (25, 26) taking into account that figures vary quite considerably between studies and some papers report higher values (24). More experiments are planned to assess protein content in cartilage by relaxometry measurements.

The changes in quadrupolar parameters such as α, η and ω_Q cannot be explained by a loss of protein, since that would only affect the amplitude of the quadrupolar peaks and not their position in the dispersion curve. These changes can be attributed to the presence of different sources of quadrupolar cross-relaxation within the cartilage, each one having different peak shapes so that the overall quadrupolar peaks observed is a sum of the contributions from the different sources. In such a situation the

depletion of only one proteoglycan would remove its contribution from the overall signal and would therefore change the shape of the resulting peaks, shifting the values of α, η and ω_Q towards the values of the other components. This also indicates that the values of the quadrupolar parameters found may reflect an average and not the property of one particular proteoglycan.

Conclusion

This study showed that FFC-NMR can detect changes between groups of normal and OA cartilages that are specific to protein content, and are expected to occur at an early stage of the disease. More studies are planned on this topic using both FFC-NMR and FFC-MRI with possible clinical applications using our whole-body FFC-MRI scanner. Imaging methods combined with quadrupolar detection may provide high sensitivity and specificity for early detection of OA by non-invasive methods.

Acknowledgements

References

1. Buckwalter JA, Mankin HJ. Articular cartilage: Tissue design and chondrocyte-matrix interactions. Instr Course Lect 1998;47:477-86.

2. Knudson CB, Knudson W. Cartilage proteoglycans. Semin Cell Dev Biol 2001;12(2):69-78.

3. Woolf AD, Pfleger B. Burden of major musculoskeletal conditions. Bull World Health Organ 2003;81(9):646-56.

4. Rogers J, Watt I, Dieppe P. Comparison of visual and radiographic detection of bony changes at the knee joint. Brit Med J 1990;300(6721):367-8.

5. Blumenkrantz G, Majumdar S. Quantitative magnetic resonance imaging of articular cartilage in osteoarthritis. Eur Cell Mater 2007;13:76-86.

6. Link TM, Stahl R, Woertler K. Cartilage imaging: Motivation, techniques, current and future significance. Eur Radiol 2007;17(5):1135-46.

7. Mankin HJ, Brandt KD. 1992. Biochemistry and metabolism of articular cartilage in osteoarthritis. In: Moskowitz RW, Howell DS, Goldberg VM, Mankin HJ. Osteoarthritis: Diagnosis and Medical/Surgical Management. 2nd ed. Philadelphia (PA): Saunders press. p 109–154.

8. Madelin G, Lee JS, Inati S, Jerschow A, Regatte RR. Sodium inversion recovery MRI of the knee joint in vivo at 7T. J Magn Reson 2010;207(1):42-52.

9. Li X, Cheng J, Lin K, Saadat E, Bolbos RI, Jokbe B, Ries MD, Horvai A, Link TM, Majumdar S. Quantitative MRI using T(1rho) and T(2) in human osteoarthritic cartilage specimens: Correlation with biochemical measurements and histology. Magn Reson Imaging 2010; 29(3):324-334.

10. Kim DK, Ceckler TL, Hascall VC, Calabro A, Balaban RS. Analysis of water-macromolecule proton magnetization transfer in articular cartilage. Magn Reson Med 1993;29:211–215.

11. Lin P-C, Reiter DA, Spencer RG. Classification of degraded cartilage through multiparametric MRI analysis. J Magn Reson 2009;201:61-71.

12. Lin P-C, Reiter DA, Spencer RG. Sensitivity and Specificity of Univariate MRI Analysis of Experimentally Degraded Cartilage. Magn Reson Med 2009;62:1311–1318.

13. Ramsey NF, Pound RV. Nuclear audiofrequency spectroscopy by resonant heating of the nuclear spin system. Phys Rev 1951;81:278-9

14. Kimmich R, Anoardo E. Field-cycling NMR relaxometry. Prog Nucl Magn Reson Spectrosc 2004;44(3-4):257, 320

15. Lurie DJ, Hutchison JMS, Bell LH, Nicholson I, Bussell DM, Mallard JR. Field-cycled proton-electron double resonance imaging of free radicals in large aqueous samples. J Magn Reson 1989;84:431-437.

16. Lurie DJ, Aime S, Baronic S, Booth NA, Broche LM, Choi CH, Davies GR, Ismail S, Ó hÓgáin D, Pine KJ. Fast Field-Cycling MRI. C R Phys 2010;11 (2):136-148

17. Alford JK, Scholl TJ, Handler WB, Chronik BA. Design and construction of a prototype high-power B_0 insert coil for field-cycled imaging in superconducting MRI systems. Concept Magn Reson B 2009;35B(1):1-10

18. Lurie DJ, Foster MA, Yeung D, Hutchison JMS. Design, construction and use of a large-sample field-cycled PEDRI imager. Phys Med Biol 1998;43:1877–1886

19. Jiao X, Bryant RG. Noninvasive measurement of protein concentration. Magn Reson Med 1996;35(2):159-61.

20. Winter F, Kimmich R. NMR field-cycling relaxation spectroscopy of bovine serum albumin, muscle tissue, micrococcus luteus and yeast. $^{14}N^{1}H$-quadrupole dips. Biochim Biophys Acta 1982;719(2):292-8.

21. Winter F, Kimmich R. Spin lattice relaxation of dipole nuclei (I=1/2) coupled to quadrupole nuclei (S=1). Mol Phys 1982;45(1):33-49

22. Sunde EP, Halle B. Mechanism of 1H-14N cross-relaxation in immobilized proteins. J Magn Reson 2010;203(2):257-73.

23. Kellgren JH, Lawrence JS. Radiological assessment of osteo-arthritis. Ann. Rheum. Dis. 1957;16:494.

24. Axelsson S, Holmlund A, Hjerpe A. Glycosaminoglycans in normal and osteoarthrotic human temporomandibular joint disks. Acta Odontol Scand 1992;50(2):113-9.

25. Grushko G, Schneiderman R, Maroudas A. Some biochemical and biophysical parameters for the study of the pathogenesis of osteoarthritis: A comparison between the processes of ageing and degeneration in human hip cartilage. Connect Tissue Res 1989;19(2-4):149-76.

26. Venn M, Maroudas A. Chemical composition and swelling of normal and osteoarthrotic femoral head cartilage. I. chemical composition. Ann Rheum Dis 1977;36(2):121-9.
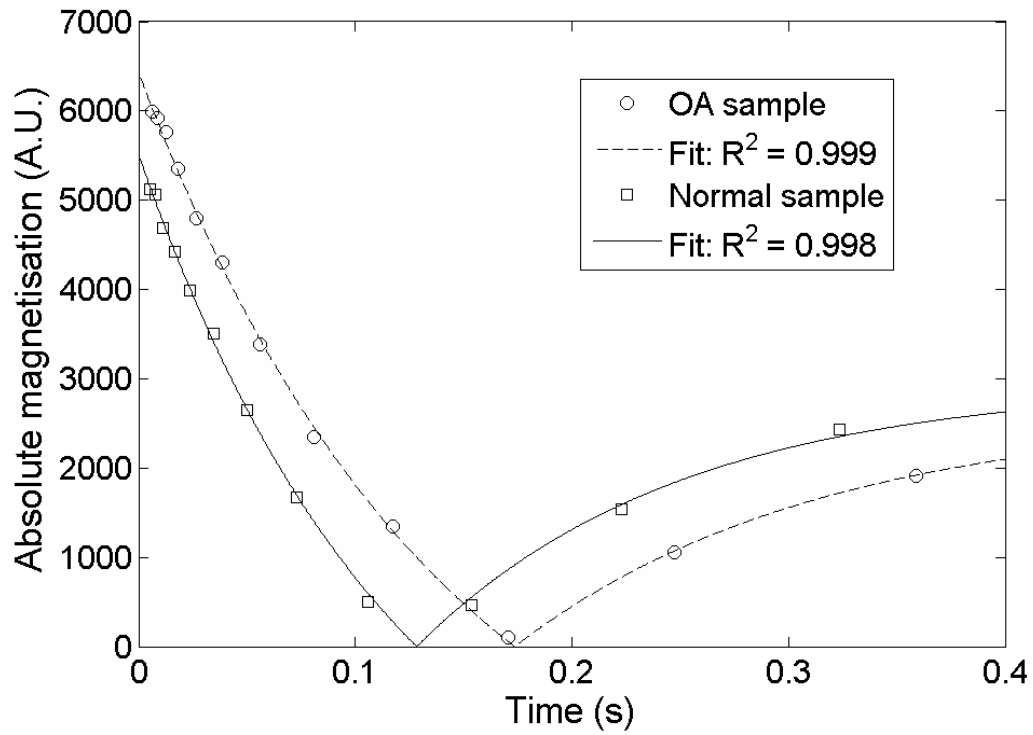
Figure 1: Magnetisation signals and fits obtained from healthy (squares) and diseased (circle) samples. Absolute values were used to prevent phase detection problem for points close to the zero line. The R2 values are representative of the entire data set.
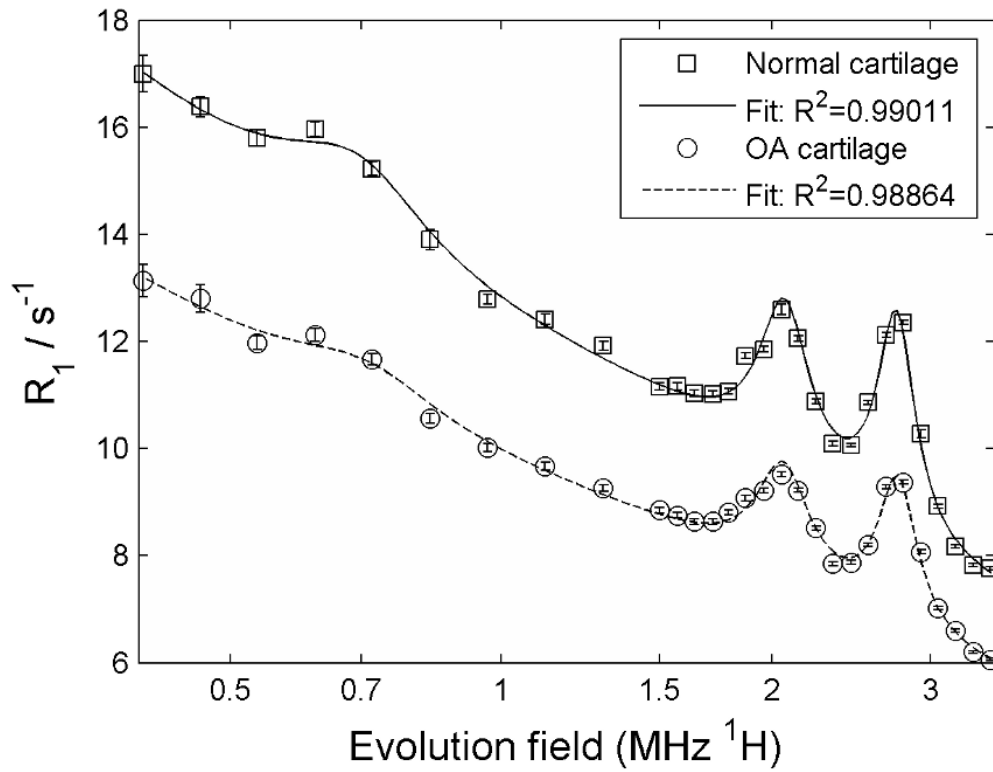
Figure 2: Typical R_1 dispersion curves obtained from normal (squares) and OA (circles) samples of cartilage. The offset between the curves is analysed later.
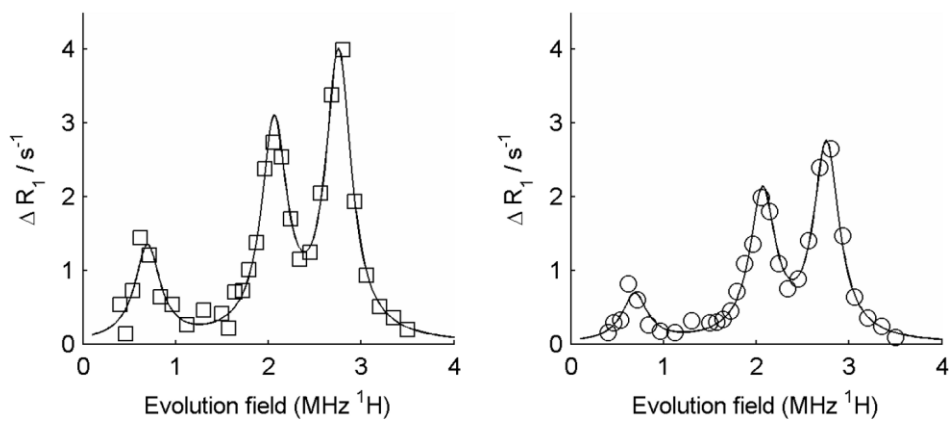

Figure 3: Quadrupolar peaks obtained by subtracting the background to the data. Left: normal cartilage; right: OA cartilage. The difference in amplitude is noticeable here.
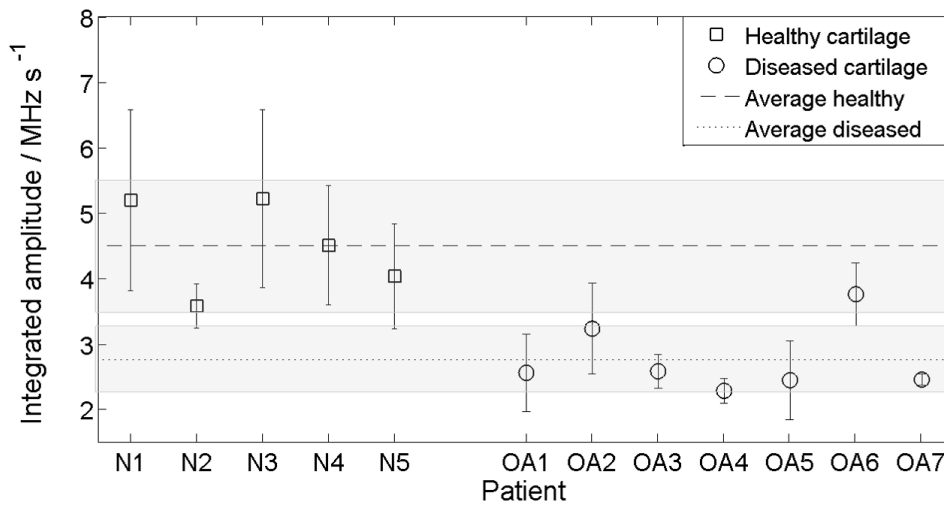
Figure 4: Distribution of the average cumulated amplitudes measured from healthy (squares) and OA (circles) patients. The population average and standard deviations are indicated by the greyed areas (error bars set to $\pm \sigma$).
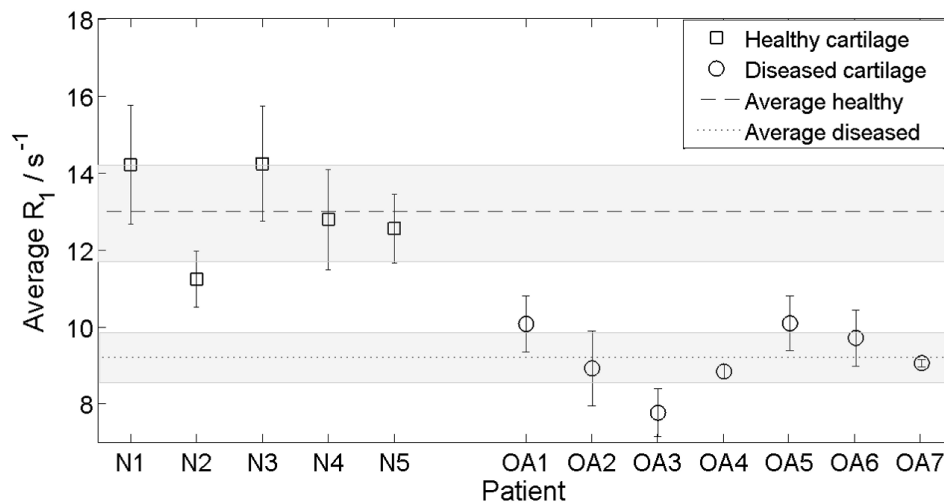

Figure 5: distribution of the average R_1 dispersion offset from healthy (squares) and OA (circles) patients. The population average and standard deviations are indicated by the greyed areas (error bars set to $\pm \sigma$).
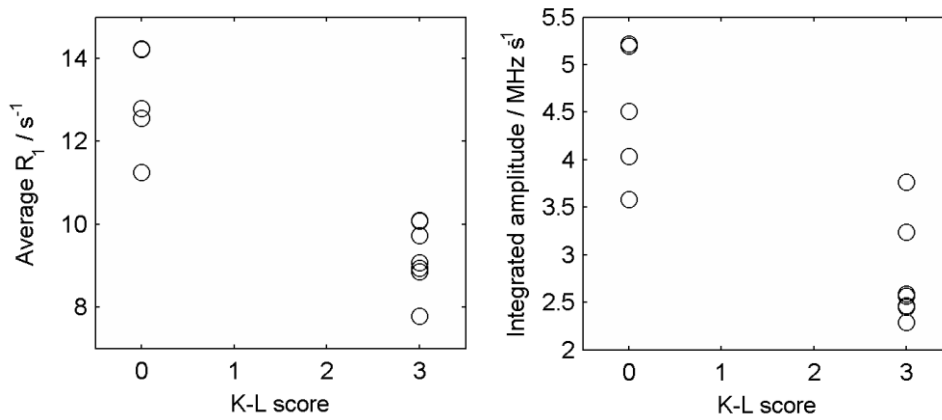
Figure 6: Comparison of the Kellgren and Lawrence (K-L) test values with, on the left graph, the average R_1 values and, on the right graph, the integrated amplitude. A Pearson's product moment correlation test on the data gave $p < 0.01$ for both data sets.

Tables:

Table 1: Distribution of the samples

Type of sample	Number of patients	Number of samples	Age (mean)	Sex	K-L test values
Normal cartilage	5	23	65	4F 1M	0
OA cartilage	7	26	61	2F 6M	3

Table 2: values provided by the model-based fitting parameters

Parameter	Value		p-value (t-test)
	Normal cartilage	OA cartilage	
α	29 ± 7	32 ± 5	<0.01
η	0.411 ± 0.010	0.420 ± 0.012	<0.01
ω_Q	3.215 ± 0.011	3.207 ± 0.010	<0.01